CrossMark

TOXICOGENOMICS

Oxidative stress and gene expression profiling of cell death pathways in alpha-cypermethrin-treated SH-SY5Y cells

Alejandro Romero[1] · Eva Ramos[1] · Irma Ares[1] · Víctor Castellano[1] ·
Marta Martínez[1] · María-Rosa Martínez-Larrañaga[1] · Arturo Anadón[1] ·
María-Aránzazu Martínez[1]

Abstract In this study, we investigated the induction of oxidative stress and apoptosis in human neuroblastoma cell line SH-SY5Y in response to alpha-cypermethrin (α-CYPER) exposure. MTT and LDH assays were carried out to assess the α-CYPER cytotoxicity. The IC_{50} value for α-CYPER was calculated to be 78.3 ± 2.98 μM for the MTT assay and 71.5 ± 3.94 μM for LDH assay. The pyrethroid α-CYPER (1–100 μM), in a dose-dependent manner, induced a significant increase in lipid peroxides measured as malondialdehyde (MDA) and in the levels of nitric oxide (NO). The neuroprotective role of three antioxidants, melatonin (MEL), Trolox and N-acetylcysteine (NAC) against α-CYPER-induced oxidative stress was examined. Compared to other antioxidants, MEL (1 μM) treatment showed the most effective protection against α-CYPER-induced lipid peroxidation and NO production. The effects of α-CYPER on gene expression profiling of cell death pathway in human neuroblastoma SH-SY5Y cells were also investigated. Of the 84 genes examined ($P < 0.001$; fold change >1.5), changes in mRNA levels were detected in 39 genes: 36 were up-regulated and 3 were down-regulated. A greater fold change reversion than 3.5-fold was observed on the up-regulated ATP6V1G2, BCL2, CASP9, FAS, GADD45A, SPATA2, SYCP2, ATG7, NFKB1, SNCA, ULK1 and JPH3 genes. The results demonstrated that α-CYPER alters the expression of apoptosis-, autophagy- and necrosis genes as well as induces oxidative stress which may lead to DNA damage. The detailed knowledge of the changes in gene expression obtained will provide a basis for further elucidating the molecular mechanisms of the α-CYPER-induced toxicity.

Abbreviations

α-CYPER	Alpha-cypermethin
AKT1	V-akt murine thymoma viral oncogene homolog 1
APAF1	Apoptotic peptidase activating factor 1
ATG3	Autophagy-related 3 homolog (S. cerevisiae)
ATG5	Autophagy-related 5 homolog (S. cerevisiae)
ATG7	Autophagy-related 7 homolog (S. cerevisiae)
ATG12	Autophagy-related 12 homolog (S. cerevisiae)
ATP6V1G2	ATPase, H + transporting, lysosomal 13 kDa, V1 subunit G2
BCL2	B cell CLL/lymphoma 2
BCL2L1	Bcl2-like 1
BIRC2	Baculoviral IAP repeat-containing 2
BMF	Bcl2 modifying factor
CASP3	Caspase 3, apoptosis-related cysteine peptidase
CASP7	Caspase 7, apoptosis-related cysteine peptidase
CASP9	Caspase 9, apoptosis-related cysteine peptidase
COMMD4	COMM domain containing 4
CTSB	Cathepsin B

✉ Arturo Anadón
aanadon@ucm.es

[1] Department of Toxicology and Pharmacology, Faculty of Veterinary Medicine, Universidad Complutense de Madrid, 28040 Madrid, Spain

CYLD	Cylindromatosis, turban tumor syndrome
DENND4A	DENN/MADD domain containing 4A
FAS	Tumor necrosis factor receptor superfamily, member 6
GADD45A	Growth arrest and DNA damage-inducible alpha
GSH	Glutathione
GRB2	Growth factor receptor-bound protein 2
HSPBAP1	HSPB (heat shock 27 kDa)-associated protein 1
HTT	Huntingtin
IGF1R	Insulin-like growth factor 1 receptor
JPH3	Junctophilin 3
MDA	Malondialdehyde tetrabutylammonium salt
MAP1LC3A	Microtubule-associated protein 1 light chain 3 alpha
MAPK8	Mitogen-activated protein kinase 8
MEL	Melatonin
NAC	N-acetylcysteine
NFKB1	Nuclear factor of kappa light polypeptide gene enhancer in B cells 1
NO	Nitric oxide
NOL3	Nucleolar protein 3 (apoptosis repressor with CARD domain)
PARP1	Poly (ADP-ribose) polymerase 1
PARP2	Poly (ADP-ribose) polymerase 2
SNCA	Synuclein, alpha (non-A4 component of amyloid precursor)
SPATA2	Spermatogenesis-associated protein 2
SQSTM1	Sequestosome 1
SYCP2	Synaptonemal complex protein 2
TP53	Tumor protein p53
TXNL4B	Thioredoxin-like 4B
ULK1	Unc-51-like kinase 1 (C. elegans)
XIAP	X-linked inhibitor of apoptosis

Introduction

Pyrethroid insecticides are potent neurotoxicants for mammals and insects. In all species tested, pyrethroids show a pattern of toxic action typical of a strongly excitant effect on the nervous system (Aldridge 1990). The principal target site for pyrethroids is defined as the voltage-dependent sodium channel in the neuronal membrane (Soderlund and Bloomquist 1989; Vijverberg and vanden Bercken 1990). Their selective toxicity seems to be mainly based on the responses of neuronal sodium channels and partially on metabolic degradation (Narahashi 1996). On the basis of different behavioral, neurophysiological and biochemical profiles, two distinct classes of pyrethroids have been identified. Type I pyrethroids are associated with hyperexcitation and fine tremors, and Type II pyrethroids, which possess an alpha-cyano group in their structure, are associated with a more complex syndrome, including clonic seizures (Verschoyle and Aldridge 1980; Aldridge 1990).

Cypermethrin (cis:trans/40:60, CAS No.: 52315-07-08) and alpha-cypermethrin (1:1 mixture of the pair of enantiomers, CAS No.: 67375-30-8) (α-CYPER), Type II pyrethroids, are extensively applied to control pests in residential and agricultural settings, to treat head lice and scabies in humans and fleas in pets, for public health vector control and for disinfection of commercial aircrafts (Anadón et al. 2009, 2013a; USEPA 2013). Despite beneficial roles in agricultural and household products, cypermethrin enters the brain, accumulates in significant quantity and exerts neurotoxicity in the non-target organisms (Malkiewicz et al. 2006; Singh et al. 2011a, b, 2012a, b). In rodents, cypermethrin induces nigrostriatal dopaminergic neurotoxicity, and if it is co-administered, it increases the neurodegenerative potential of toxic chemical (Mun et al. 2005; Elwan et al. 2006; Nasuti et al. 2007). Pyrethroids also induce chronic effects in human, including neurotoxicity (Power and Sudakin 2007). Evidence has also showed that pyrethroids could induce various toxic effects including development and reproductive effects, genotoxicity and enzyme induction, among others (Amer et al. 1993; Giri et al. 2003; Power and Sudakin 2007; Anadón et al. 2013b).

Currently, oxidative stress is among the most important subjects in pesticide toxicology (Zhao et al. 2009; Mansour and Mossa 2010; Romero et al. 2016). It has been reported that cypermethrin has the potential to induce oxidative stress (Kale et al. 1999; Giray et al. 2001; Patel et al. 2006). The mechanism by which cypermethrin induces oxidative stress and DNA damage has received attention. To date, in vitro and in vivo studies (Jin et al. 2011a, b, c; Singh et al. 2011b; Tiwari et al. 2012; Maurya et al. 2012) were performed, showing that cypermethrin alters the expression of stress- and toxicity-related genes.

Because, the pyrethroid α-CYPER is considered as one of the more used pyrethroid insecticides worldwide, and no oxidative stress and toxicity pathway studies have been described with this formulation; in the present study, the possible link between oxidative stress and cell death pathways, crucial in α-CYPER toxicity, was investigated. This in vitro study was undertaken (1) to characterize the concentration-dependent cytotoxicity of α-CYPER using cell viability assays and to determine the different protective roles of the selected antioxidant substances, MEL, Trolox and NAC, on lipid peroxidation and NO formation and (2) to analyze by PCR array profiles of the expression of key genes involved in apoptosis, autophagy and necrosis after α-CYPER exposure.

In this in vitro experiment, we used the cell line SH-SY5Y which has been widely used in experimental neurological studies in particular analysis of neuronal

differentiation, metabolism and function related to neurodegenerative and neuroadaptive processes, neurotoxicity and neuroprotection (Pahlman 1990). SH-SY5Y cells in both undifferentiated and differentiated states express a number of dopaminergic neuronal markers making them an exemplary in vitro system for the study of neurotoxicity in dopaminergic neurons as well as for drugs, which are known to produce primary effects through activation of dopamine receptors (Kovalevich and Langford 2013). This cell line is a reliable model for studying the neurotoxic effects of pesticides and for elucidating the mechanisms of induced neurotoxicity from the aspect of apoptosis. Moreover, compared to other neuronal cell line, it is more vulnerable to reactive oxygen species (ROS)-mediated oxidative injury (Romero et al. 2010).

Materials and methods

Chemicals and reagents

The Type II pyrethroid α-cypermethrin (α-CYPER) is a 1:1 mixture of the pair of enantiomers(R)-α-cyano-3-phenoxybenzyl(1S,3S)-3-(2,2-dichlorovinyl)-2,2-dimethyl cyclopropanecarboxylate, and (S)-α-cyano-3-phenoxybenzyl(1R,3R)-3-(2,2-dichlorovinyl)-2,2-dimethyl cyclopropanecarboxylate (CAS No.: 67375-30-8) (molecular formula $C_{22}H_{19}C_{12}NO_3$; molecular weight 416.3 g/mol; >99 % purity) was provided by BASF Española S.L. (Barcelona, Spain). The compounds 3-[4,5 dimethylthiazol-2-yl]-2,5-diphenyl-tetrazolium bromide (MTT), melatonin (N-acetyl-5-methoxytryptamine) (MEL), N-acetyl-cysteine (NAC), Trolox [(±)-6-hydroxy-2,5,7,8-tetramethylchroman-2-carboxylic acid], malondialdehyde tetrabutylammonium salt (MDA) and F-12 nutrient mixture were obtained from Sigma (St Louis, MO, USA). Fetal bovine serum (FBS), penicillin and streptomycin were obtained from Invitrogen (Madrid, Spain). All other chemicals were reagent grade of the highest laboratory purity available.

Culture of SH-SY5Y cells

Human dopaminergic neuroblastoma SH-SY5Y cells were maintained in a 1:1 mixture of F-12 nutrient mixture and Eagle's minimum essential medium (EMEM) supplemented with 15 non-essential amino acids, sodium pyruvate (1 mM), 10 % heat-inactivated FBS, 100 units/ml penicillin and 100 μg/ml streptomycin. Cultures were seeded into flasks containing supplemented medium and maintained at 37 °C in a humidified atmosphere of 5 % CO_2 and 95 % air. For assays, SH-SY5Y cells were subcultured in 96-well plates at a seeding density of 8×10^4 cells per well. Cells were treated with the drugs before confluence

in F-12/EMEM with 1 % FBS. A vehicle group containing 0.1 % dimethyl sulfoxide (DMSO) was employed in parallel for each experiment. All SH-SY5Y cells used in this study were used at a low passage number (<13).

MTT assay and cell viability

Cell viability, virtually the mitochondrial activity of living cells, was measured by quantitative colorimetric assay with MTT, as described previously (Denizot and Lang 1986). Briefly, 50 μl of the MTT labeling reagent, at a final concentration of 0.5 mg/ml, was added to each well at the end of the incubation period, and the plate was placed in a humidified incubator at 37 °C with 5 % CO_2 and 95 % air (v/v) for an additional 2-h period. Metabolically active cells convert the yellow MTT tetrazolium compound to a purple formazan product. The insoluble formazan was dissolved with DMSO; colorimetric determination of MTT reduction was measured at 540 nm. Control cells treated with F-12/EMEM were taken as 100 % viability.

Lactate dehydrogenase (LDH) assay

The possible cytotoxic effect of α-CYPER exposure on SH-SY5Y cells was also evaluated by measuring LDH leakage into the extracellular fluid. LDH is a stable cytoplasmic enzyme present in all cells. It is rapidly released into the cell culture supernatant upon damage of the plasma membrane. After α-CYPER exposition (24 h) at several concentrations, samples were collected to estimate extracellular LDH as indication of cell death. LDH activity was spectrophotometrically measured using a Cytotoxicity Cell Death kit (Roche-Boehringer, Mannheim, Germany) according to the manufacturer's indications. Total LDH activity was defined as the sum of intracellular and extracellular LDH activity; total LDH (intracellular plus extracellular) was normalized as 100 %; then, the amount of LDH released to the extracellular medium was expressed as percentage of this total value. LDH activity was measured spectrophotometrically at 490–620 nm, using a microplate reader (Biochrom ASYS UVM 340, Cambridge, UK).

Determination of lipid peroxidation

Malondialdehyde (MDA) is a breakdown product of the oxidative degradation of cell membrane lipids, and it is generally considered an indicator of lipid peroxidation. In this study, we evaluated lipid peroxidation induced by α-CYPER (1, 3, 10, 30, 60 and 100 μM) after 24-h incubation period. We selected 24-h incubation period because at this time the maximum MDA levels without necrosis were found (data not shown). Intracellular MDA production was quantified using a thiobarbituric acid reactive substance

(TBARS) assay kit (Cell Biolabs Inc., San Diego, CA). Briefly, 1×10^6 cells per well were seeded in a six-well plate, then collected in 200 µl of culture medium and sonicated for 3×5 s intervals at 40 V over ice. SDS Lysis solution (100 µl) was added to the sample solution and the MDA standards in a microcentrifuge tube and mixed thoroughly. Then, 250 µl of TBA reagent was added to each sample and standard to be tested and incubated at 95 °C for 45–60 min. Each sample and standard (200 µl) were loaded (in duplicate) into a clear 96-well plate, and the absorbance at 532 nm was recorded using a microplate reader (Biochrom ASYS UVM 340, Cambridge, UK). The content of MDA was calculated for each sample from a standard curve.

Nitrite measurement

Nitric oxide (NO) has been identified as a mediator of cytokine action in various cell types. NO is an intra- and intercellular messenger that mediates a variety of important physiological processes (Moncada et al. 1991). Changes in NO production were measured indirectly as the accumulation of nitrites (the end product of NO metabolism) in the medium using Griess assay as previously described (Bauche et al. 1998). Neuroblastoma SH-SY5Y cells were incubated with α-CYPER (1, 3, 10, 30, 60 and 100 µM). After incubation period, 100 µl of the culture supernatant reacted with 100 µl Griess reagent (1 % sulfanilamide, 0.1 % naphthylethylenediamine dihydrochloride and 2–5 % H_3PO_4) for 10 min at room temperature. The concentration of nitrite was measured by spectrophotometry (Biochrom ASYS UVM 340, Cambridge, UK) at 540 nm, and the nitrite concentration was calculated using a standard curve of sodium nitrite.

RNA extraction and purification

Neuroblastoma SH-SY5Y cells were co-incubated with α-CYPER (60 µM) for 24 h with or without MEL (1 µM). Total RNA was extracted using the Trizol reagent method (Invitrogen) and purified using RNeasy MinElute Cleanup Kit according to the manufacturer's protocol (Qiagen, Valencia, CA). The final RNA concentration and purity were determined using a NanoDrop 2000c spectrophotometer (ThermoFisher Scientific, Madrid, Spain), and the integrity of total RNA samples was assessed using an Experion LabChip Gel (Bio-Rad, Madrid, Spain). The samples showing A_{260}/A_{280} ratios between 1.9 and 2.1 and having RNA integrity number above 7.5 were used for further analysis.

Real-time PCR array analysis

First-strand cDNA was synthesized with 1000 ng of cRNA using a PCR array first-strand synthesis kit (C-02;

SABiosciences Inc.). The Human Cell Death Pathway Finder PCR Array (PAHS-212Z) was used to analyze mRNA levels of 84 key genes involved in cell death, in a 96-well format, according to the manufacturer's instructions (SABiosciences Inc.). Reactions were run on a Real-Time PCR system, Bio-Rad CFX96, using Real-Time SYBR Green PCR master mix PA-012 (SABiosciences Inc.). The thermocycler parameters were 95 °C for 10 min, followed by 40 cycles of 95 °C for 15 s and 60 °C for 1 min. Relative changes in gene expression were calculated via SuperArray PCR Array Data Analysis software using the Ct (cycle threshold) method with normalization of the raw data to several housekeeping genes. The expression data are presented as real change multiples.

Ingenuity pathway analysis (IPA)

Datasets representing genes with altered expression profile derived from real-time PCR array analyses were imported into the Ingenuity Pathway Analysis Tool (IPA Tool; Ingenuity H Systems, Redwood City, CA, USA; http://www.ingenuity.com). In IPA, differentially expressed genes are mapped to genetic networks available in the Ingenuity database and then ranked by score. The basis of the IPA program consists of the Ingenuity Pathway Knowledge Base (IPKB) which is derived from known functions and interactions of genes published in the literature. Thus, the IPA Tool allows the identification of biological networks, global functions and functional pathways of a particular dataset. The program also gives the significance value of the genes, the other genes with which it interacts, and how the products of the genes directly or indirectly act on each other, including those not involved in the microarray analysis. The networks created are ranked depending on the number of significantly expressed genes they contain and also list diseases that were most significant. A network is a graphical representation of the molecular relationships between molecules. Molecules are represented as nodes, and the biological relationship between two nodes is represented as an edge (line). All edges are supported by at least 1 reference from the literature, from a textbook or from canonical information stored in the Ingenuity Pathways Knowledge Base.

Datasets representing genes with altered expression profile derived from real-time PCR array analyses with $\geq \pm 1.5$-fold were uploaded into the IPA Tool. Canonical pathways and network analysis in IPA were used to identify the genes that were altered by α-CYPER treatment.

Statistical analysis

At least three replicates for each experimental condition were performed, and the presented results were representative of these replicates. Data are represented as mean ± standard error of the mean (SEM). Comparisons

between experimental and control groups were performed by one-way ANOVA followed by the Newman–Keuls post hoc test. Statistical difference was accepted when $P < 0.05$, and a fold change cutoff of 1.5 was selected. Subsequent statistical analyses were performed with the GraphPad Prism 5 software package (version 5.02, GraphPad Software Inc.). IC_{50} value was calculated by concentration–response (sigmoidal fitting) with OriginPro 7.5 software.

Results

Effect of α-CYPER on SH-SY5Y cell viability MTT and LDH assays

In order to evaluate cell survival, we used MTT assay. As Fig. 1a illustrates, the difference between data of vehicle-treated cells (0.1 % DMSO) and control cells was not statistically significant. A 24-h incubation period with α-CYPER at increasing concentrations (0.01–1000 μM) reduced cell viability in a concentration-dependent manner compared with vehicle-treated cells (control negative). The IC_{50} value for α-CYPER was calculated to be 78.3 ± 2.98 μM.

We also examined whether exposure to α-CYPER induced cell death by assessing LDH leakage. SH-SY5Y cells incubated for a 24-h period with α-CYPER (0.01–1000 μM) produced significant elevations in LDH leakage (Fig. 1b). The IC_{50} value for α-CYPER was calculated to be 71.5 ± 3.94 μM.

At 60 μM, α-CYPER showed cytotoxicity by MTT and LDH assays (Fig. 1a, b). This value was equivalent to 1/4 of the LD_{50} oral value in Wistar rats of α-CYPER (data not shown). Therefore, this was the concentration selected for the following experiments.

Effect of α-CYPER on SH-SY5Y cell viability after co- and post-incubation with antioxidants

MEL (0.01, 0.1 and 1 μM), Trolox (0.1, 0.3 and 1 μM) and NAC (100, 500 and 1000 μM) exhibited differences preventing decreases in cell viability caused by α-CYPER (60 μM) (Fig. 2). We found that the effects of MEL, Trolox and NAC were concentration-dependent. Our results demonstrated that both co-incubation (Fig. 2a–c) and post-incubation (Fig. 2d–e) with MEL (1 μM), Trolox (1 μM) and NAC (1000 μM), significantly protected against cytotoxicity induced by α-CYPER (60 μM) in SH-SY5Y cells.

Effect of antioxidants on lipid peroxidation in α-CYPER-exposed SH-SY5Y cells

MDA is one of the most important intermediates produced during lipid peroxidation. Figure 3a shows the lipid peroxidation induced by α-CYPER (1, 3, 10, 30, 60 and 100 μM)
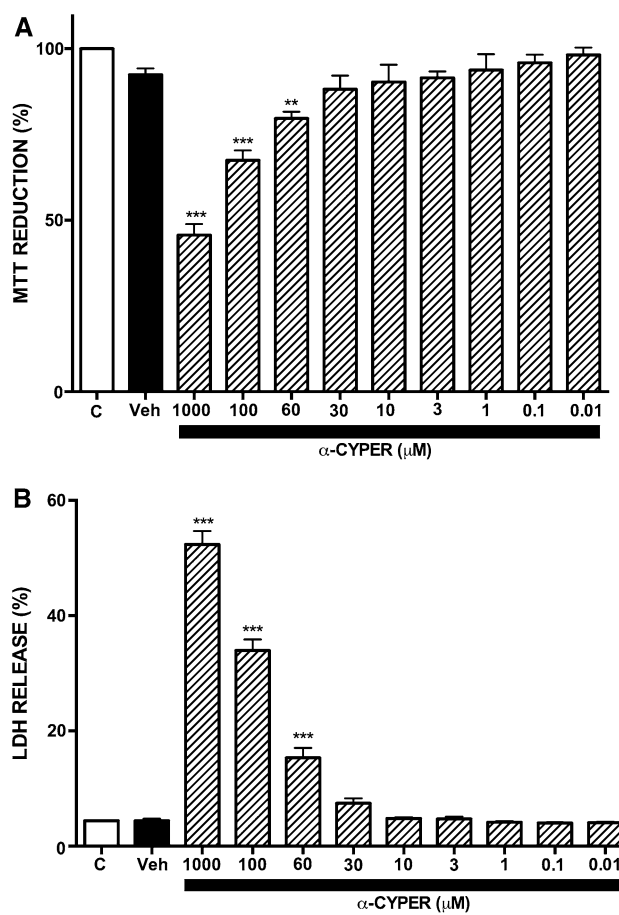

Fig. 1 Cytotoxicity induced by α-CYPER on SH-SY5Y cell viability after 24-h incubation period. Experiments were run in parallel as the protocol describes. Cell viability was measured as MTT reduction (**a**) or as LDH release (**b**) (ordinate), and data were normalized as % control (*white column*). Cells treated with DMSO (0.1 %) were the negative control [vehicle (Veh), *black column*]. Data represent the mean $\pm$ SEM of five independent experiments in triplicate. **$P < 0.01$ and ***$P < 0.001$ compared to Veh

after 24-h incubation period. Incubation with α-CYPER for 24 h induced, in a dose-dependent manner, a significant increase in MDA levels compared to vehicle group (Veh). α-CYPER 60 μM was the lower concentration that caused a significant twofold increase in MDA levels. Figure 3b shows the lipid peroxidation induced by α-CYPER (60 μM) after 24-h co-incubation with the antioxidants MEL (1 μM), Trolox (1 μM) and NAC (1 mM). MEL (1 μM), but not Trolox (1 μM) nor NAC (1 mM), provided a significant decrease (29.2 %) of MDA levels induced by α-CYPER.

Effect of antioxidants on nitric oxide (NO) production in α-CYPER-exposed SH-SY5Y cells

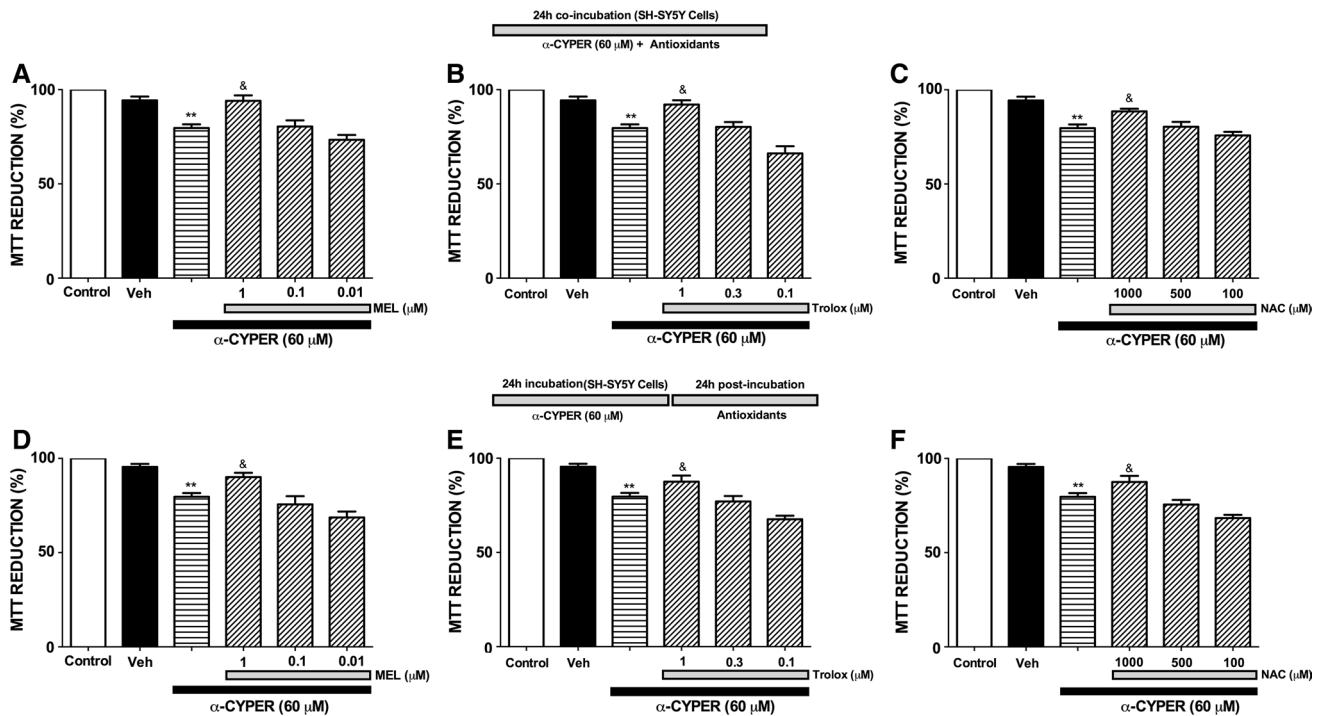A marked increase in NO is detrimental of many pathological conditions; furthermore, excessive NO can trigger

Fig. 2 Cytoprotection of MEL, Trolox and NAC after 24-h co-incubation (**a**, **b** and **c**) and post-incubation (**d**, **e** and **f**) period against cell death elicited by α-CYPER (60 μM). The protocol used to evoke cytotoxicity on SH-SY5Y cells is described in figure. Cells treated with DMSO (0.1 %) were the negative control [vehicle (Veh), *black column*]. Data represent the mean ± SEM of five independent experiments in triplicate. **P < 0.01 compared to Veh. [&]*P* < 0.05 compared to α-CYPER in the absence of antioxidants

a neurotoxic cascade. As shown in Fig. 4a, in cells exposed to α-CYPER (1, 3, 10, 30, 60 and 100 μM) after 24-h incubation period, we found, in a dose-dependent manner, a significant increase in NO production. α-CYPER 60 μM was the lower concentration that caused a significant 3.5-fold increase in NO levels (Fig. 4a). After a 24-h co-incubation period with the antioxidants MEL (1 μM), Trolox (1 μM) and NAC (1 mM), the NO production induced by α-CYPER (60 μM) was significantly reduced in 54.7, 31.25 and 25 %, respectively (Fig. 4b).

Gene expression profiles comparison between control and α-CYPER group

Gene expression profiling of cell death pathways to α-CYPER (60 μM) and control samples (0.1 % DMSO) was performed using real-time RT-PCR. The gene expression profiles of α-CYPER were significantly different from control; thus, set of genes were successfully clustered (Fig. 5).

Genes were considered up- or down-regulated if the average fold change in expression was 1.5 or above in three different experiments. Of the 84 genes examined (*P* < 0.001; fold change >1.5), changes in mRNA levels were detected in 39 genes: 36 were up-regulated and 3

were down-regulated. The differentially expressed genes are listed in Table 1. Of these genes, the expression levels of AKT1; APAF1; ATG3; ATG5; ATG7; ATG12; ATP6V1G2; BCL2; BCL2L1; BIRC2; BMF; CASP3; CASP7; CASP9; COMMD4; CTSB; CYLD; DENND4A; FAS; GADD45A; HSPBAP1; HTT; IGF1R; JPH3; MAP1LC3A; MAPK8; NFKB1; NOL3; PARP2; SNCA; SPATA2; SQSTM1; SYCP2; TXNL4B; ULK1; and XIAP genes were up-regulated in the cells exposed to α-CYPER (60 μM), to levels that were 2.80; 2.30; 1.98; 2.54; 3.87; 2.12; 3.99; 3.62; 2.85; 3.17; 2.07; 2.82; 2.09; 3.70; 2.60; 3.16; 1.92; 1.80; 7.65; 7.09; 3.42; 1.62; 1.67; 5.15; 3.24; 1.65; 4.41; 1.81; 1.61; 4.68; 4.32; 3.04; 3.94; 2.47; 6.50; and 2.48, times higher, respectively, than those in control cultures (*P* < 0.001; Table 1). In addition, the expression levels of GRB2, PARP1 and TP53 genes were significantly down-regulated in the cells exposed to α-CYPER (60 μM) to levels that were 1.90; 2.20 and 2.29 times lower, respectively, than those in control cultures (*P* < 0.001; Table 1).

Ingenuity pathway analysis (IPA)

To investigate possible biological interactions of differently regulated genes, datasets representing genes with altered expression profile derived from real-time PCR array
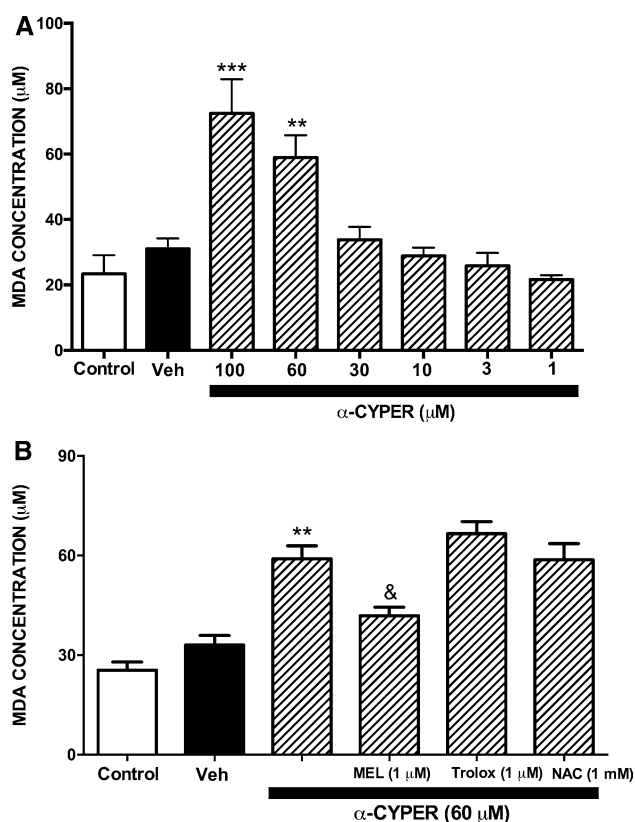
Fig. 3 MDA production in SH-SY5Y cells induced by α-CYPER after 24-h exposure (**a**). Effect of antioxidants MEL (1 μM), Trolox (1 μM) and NAC (1 mM) on MDA levels induced by α-CYPER (60 μM) after 24-h co-incubation period (**b**). Cells treated with DMSO (0.1 %) were the negative control [vehicle (Veh), *black column*]. Data represent the mean $\pm$ SEM of five independent experiments in triplicate. **$P < 0.01$ and ***$P < 0.001$ compared to Veh. &$P < 0.05$ compared to α-CYPER in the absence of antioxidants

Fig. 4 NO production in SH-SY5Y cells induced by α-CYPER after 24-h exposure (**a**). Effect of antioxidants MEL (1 μM), Trolox (1 μM) and NAC (1 mM), on NO production induced by α-CYPER (60 μM) after 24-h co-incubation period (**b**). Cells treated with DMSO (0.1 %) were the negative control [vehicle (Veh), *black column*]. Data represent the mean $\pm$ SEM of five independent experiments in triplicate. **$P < 0.01$ and ***$P < 0.001$ compared to vehicle (Veh). &$P < 0.05$ and &&$P < 0.01$ compared to α-CYPER in the absence of antioxidants

analyses were imported into the Ingenuity Pathway Analysis Tool. The list of differentially expressed genes analyzed by IPA revealed 5 significant networks after α-CYPER (60 μM) exposure. Figure 6a represents the list of top 5 networks identified by IPA. Of these networks, Cellular Assembly and Organization, Cell Morphology, Cellular Function and Maintenance were the highest rated networks with 60 focus molecules and the significance score of 36 (Fig. 6e). The score is the probability that a collection of genes equal to or greater than the number in a network could be achieved by chance alone. A score of 3 indicates a 1/1000 chance that the focus genes are in a network not due to random chance. The IPA analysis also groups the differentially expressed genes into biological mechanisms that are related to Cell Death and Survival, Cellular Function and Maintenance, Cell Morphology, DNA Replication, Recombination and Repair and Cellular assembly and Organization with 60 focus molecules for Cell Death and Survival (Fig. 6b). The main signaling canonical pathway
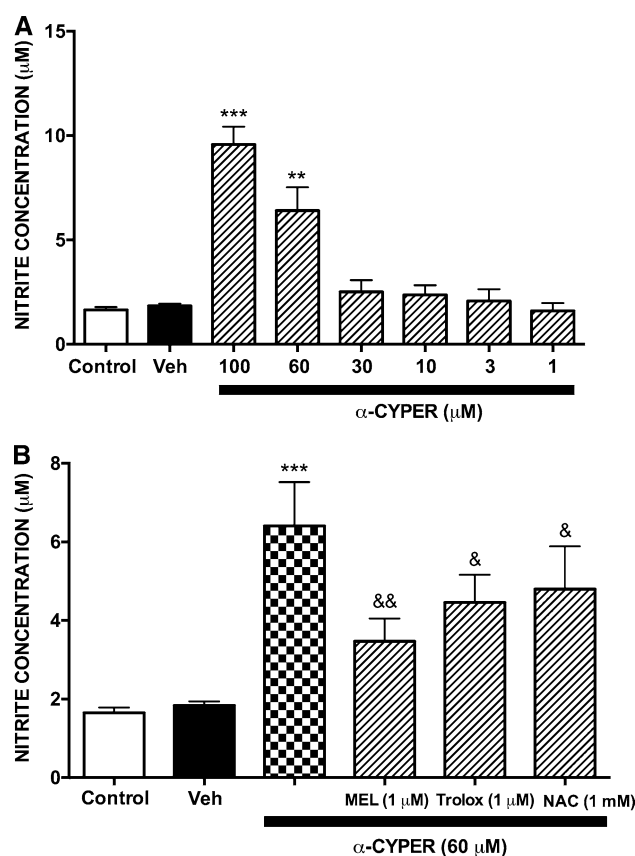
was apoptosis signaling (Fig. 6c). The genes up- and down-regulated on apoptosis signaling canonical pathway and on the top network were represented for α-CYPER (Fig. 6d, e). Top network for α-CYPER summarizes the highest number of connections among the larger number of differentially expressed genes, being mainly related to cell death process.

Discussion

Several studies have evaluated the neurotoxicity induced by cypermethrin. This pyrethroid exerts its neurodegenerative effects by involving multiple biological pathways, including oxidative stress, inflammation, cellular energy, xenobiotic metabolism and microglial activation (Casco et al. 2006; Tiwari et al. 2010, 2012; Jin et al. 2011b; Singh et al. 2011b). However, little is known about the cell death
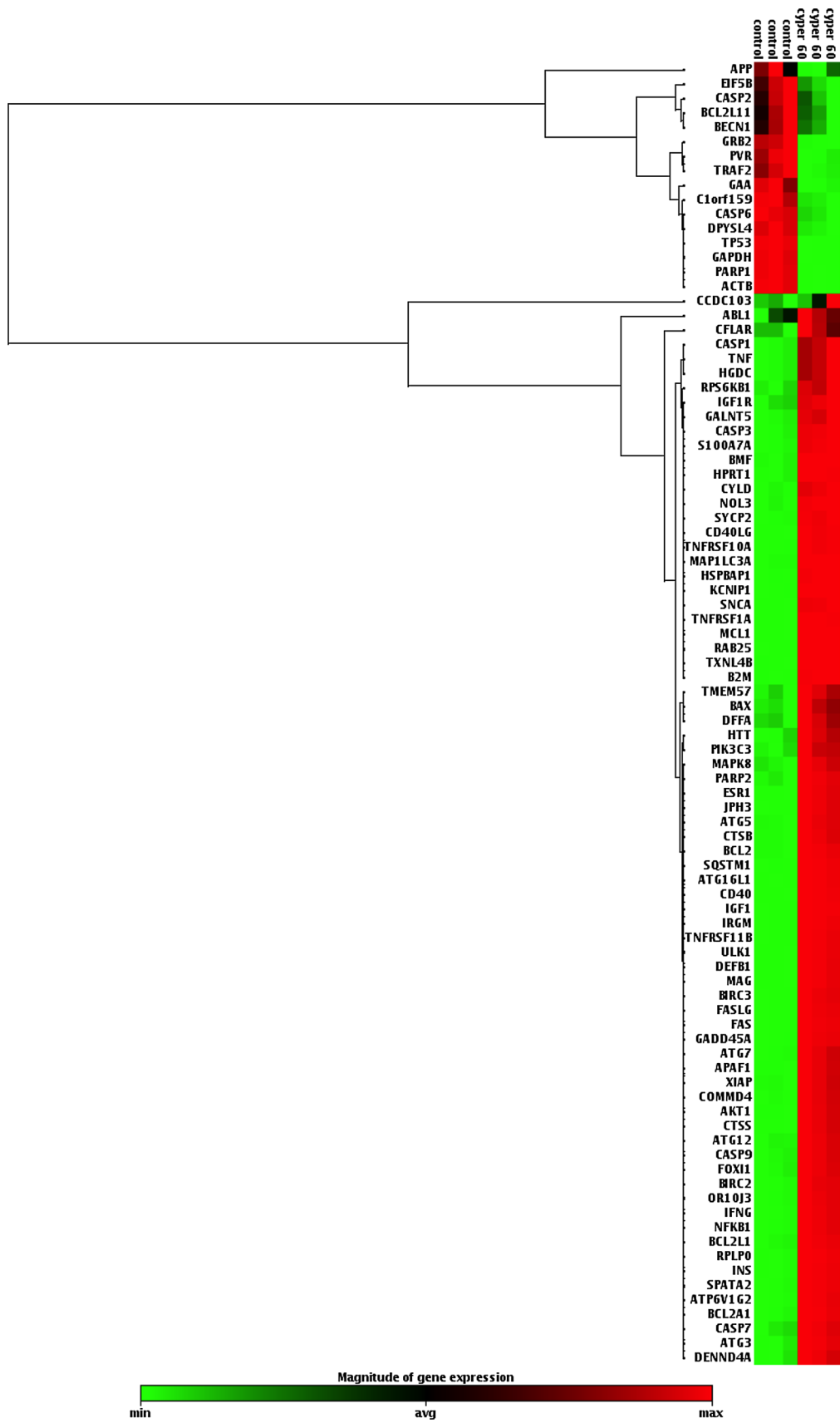
◄**Fig. 5** Hierarchical clustering of the relative expression of the 84 cell death-related genes analyzed. *Green* represents genes whose transcription is down-regulated, while *red* represents genes down-regulated (fold change 1.5 or above in gene expression threshold) after α-CYPER (60 μM) treatment (color figure online)

mechanisms concerning to α-CYPER. To our knowledge, this is the first study to examine the effect of α-CYPER on three death processes: apoptosis, autophagy and necrosis.

The effect of cytotoxicity of α-CYPER appeared at the concentration of 60 μM. Concentrations from 0.01 to 30 μM of α-CYPER had no effect on cell viability (MTT and LDH leakage), similar results than those observed previously for the pyrethroid cypermethrin in SH-SY5Y cells (Raszewski et al. 2015). The present study also found that exposure to α-CYPER introduces significant oxidative stress in SH-SY5Y cells as was evident by the elevation of the MDA and NO levels, >50 % of enhancement after 24 h of the exposure of 60 μM of α-CYPER and a dose equivalent to 25 % LD_{50} of α-CYPER. The results of Giray et al.

(2001) are in accordance with our findings; they showed doses lower 20 % LD_{50} of cypermethrin, and no lipid peroxidation was observed (Giray et al. 2001). To assay a possible protection against oxidative injury, antioxidant substances were tested: melatonin (MEL), a potent free radical scavenger and neuroprotective drug (Rodríguez et al. 2004), Trolox, a cell-permeative analog of vitamin E, which inhibits ROS-induced generation of lipid peroxyl radicals (Cort et al. 1975), and N-acetylcysteine (NAC), a free radical scavenger that acts as a cysteine donor and maintains or even increases the intracellular levels of glutathione (Li et al. 2007). MEL was the most active compound to maintain better the cell viability. The smaller protective effect of Trolox and NAC compared to MEL might be due to the fact that the antioxidant capacity of MEL also includes the indirect effect of up-regulating several antioxidative enzymes and down-regulating pro-oxidant enzymes, in particular 5- and 12-lipo-oxygenases and NO synthases (Pandi-Perumal et al. 2006). MEL influences a number of physiological processes such as temperature, seasonal reproduction and

Table 1 Results from RT^2 Profiler™ PCR Array targeting select genes associated with apoptosis, autophagy and necrosis

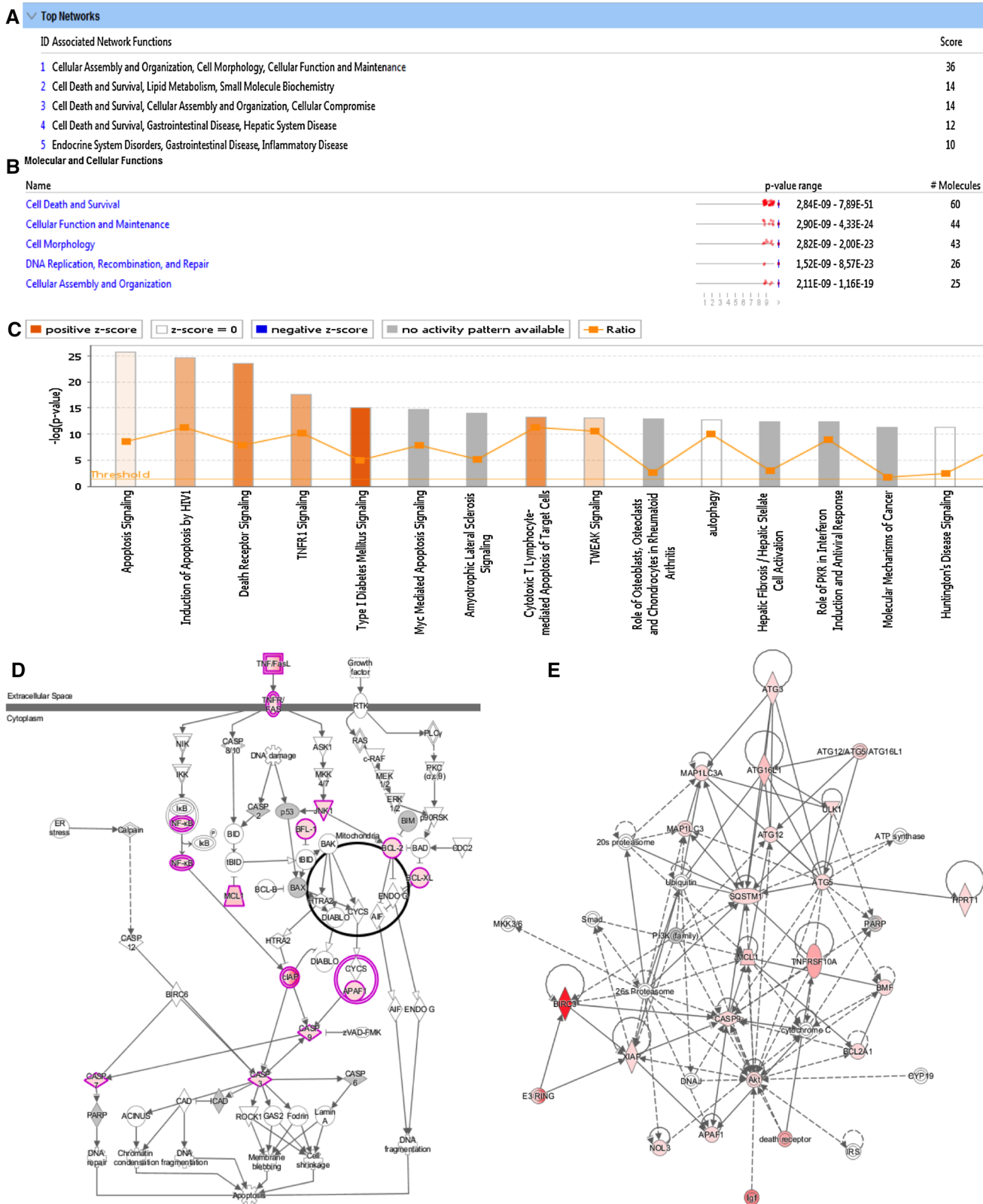| Gene symbol	GenBank accession no.	Fold change α-CYPER	Gene symbol	GenBank accession no.	Fold change α-CYPER	Gene symbol	GenBank accession no.	Fold change α-CYPER
Apoptosis			*Autophagy*			*Necrosis*		
AKT1	NM_005163	2.80	ATG3	NM_022488	1.98	BMF	NM_033503	2.07
APAF1	NM_001160	2.30	ATG5	NM_004849	2.54	COMMD4	NM_017828	2.60
ATP6V1G2	NM_130463	3.99	ATG7	NM_006395	3.87	CYLD	NM_015247	1.92
BCL2[a]	NM_000633	3.62	ATG12	NM_004707	2.12	DENND4A	NM_005848	1.80
BCL2L1	NM_138578	2.85	CTSB	NM_001908	3.16	GRB2	NM_002086	−1.90
BIRC2	NM_001166	3.17	HTT	NM_002111	1.62	HSPBAP1	NM_024610	3.42
CASP3[a]	NM_004346	2.92	MAP1LC3A	NM_181509	3.24	JPH3	NM_020655	5.15
CASP7	NM_001227	2.09	MAPK8	NM_002750	1.65	PARP1	NM_001618	−2.20
CASP9	NM_001229	3.70	NFKB1	NM_003998	4.41	PARP2	NM_005484	1.61
FAS[a]	NM_000043	7.65	SNCA	NM_000345	4.68	TXNL4B	NM_017853	2.47
GADD45A	NM_001924	7.09	SQSTM1	NM_003900	3.04			
IGF1R	NM_000875	1.67	ULK1	NM_003565	6.50			
NOL3	NM_003946	1.81						
SPATA2[b]	NM_006038	4.32						
SYCP2[b]	NM_014258	3.94						
TP53[a]	NM_000546	−2.29						
XIAP	NM_001167	2.48						

SH-SY5Y cells were treated with α-CYPER (60 μM) or DMSO (0.1 %) as the carrier control

Data for gene expression represent fold change mean of three independent experiments in which specific gene expression was compared to control

$P < 0.001$ compared to the control

[a] Genes related to both apoptosis and autophagy pathways

[b] Genes related to both apoptosis and necrosis pathways

A Top Networks

ID	Associated Network Functions	Score
1	Cellular Assembly and Organization, Cell Morphology, Cellular Function and Maintenance	36
2	Cell Death and Survival, Lipid Metabolism, Small Molecule Biochemistry	14
3	Cell Death and Survival, Cellular Assembly and Organization, Cellular Compromise	14
4	Cell Death and Survival, Gastrointestinal Disease, Hepatic System Disease	12
5	Endocrine System Disorders, Gastrointestinal Disease, Inflammatory Disease	10

B Molecular and Cellular Functions

Name		p-value range	# Molecules
Cell Death and Survival		2,84E-09 - 7,89E-51	60
Cellular Function and Maintenance		2,90E-09 - 4,33E-24	44
Cell Morphology		2,82E-09 - 2,00E-23	43
DNA Replication, Recombination, and Repair		1,52E-09 - 8,57E-23	26
Cellular Assembly and Organization		2,11E-09 - 1,16E-19	25

immune response and recently is believed to play an anti-tumoral role in several types of cancers. MEL may be a pro-apoptotic and pro-necrotic agent for pancreatic cancer cells via its modulation of BCL2/BAX balance (Xu et al. 2013). Although MEL seems to have a great diversity of actions on gene regulation that require further clarification,

◄**Fig. 6** Ingenuity pathways analysis (IPA) summary of α-CYPER (60 μM) treatment. To investigate possible interactions of differently regulated genes, datasets representing 84 genes with altered expression profile obtained from real-time PCR arrays were imported into the Ingenuity Pathway Analysis Tool and the following data are illustrated: **a** The list of top five molecular and cellular functions with their respective scores obtained from IPA. **b** The list of top five biofunctions with their respective scores obtained from IPA. **c** Toxicology pathway list in IPA analysis. The x-axis represents the top toxicology functions as calculated by IPA based on differentially expressed genes that are highlighted and the y-axis represents the ratio of number of genes from the dataset that map to the pathway and the number of all known genes ascribed to the pathway. The orange line represents the threshold of $P < 0.05$ as calculated by Fisher's test. **d** Toxicology pathway obtained in IPA. **e** Most highly rated network in IPA analysis. The genes that are shaded were determined to be significant from the statistical analysis. A *solid line* represents a direct interaction between the two gene products, and a *dotted line* means there is an indirect interaction. *Gray* represents down-regulation, while *red* depicts up-regulation. *White* represents no change in expression (color figure online)

it is suggested that MEL might be a possible agent benefiting the treatment of α-CYPER toxicity. Further research is necessary to determine whether MEL could be useful for protecting the neurotoxicity related to α-CYPER exposure.

The second objective of this study was to analyze by PCR array profiles of the expression of key genes involved in apoptosis, autophagy and necrosis after α-CYPER exposure. Real-time PCR array system is the ideal tool for analyzing the expression of a focused panel of genes, and the IPA analysis allows the identification of biological networks, global functions and functional pathways of a particular dataset. In the RNA, samples from treated α-CYPER cells observed a greater or lower fold change than 1.5 in comparison with the control (Table 1) in expression of the 39 genes involvement in these biological pathways. In our in vitro study, we demonstrate that α-CYPER may exert its cell death effects involving apoptosis, necroptosis and autophagy pathways.

Apoptosis is a form of cellular suicide that is widely observed in nature. This process can be triggered by a variety of stimuli, including cytokines, hormones, viruses and toxic insults. The step of apoptosis regulation that is controlled by the BCL-2 family appears to be the most general final commitment step for the decision between cell life and death. BCL-2 family members are major regulators of mitochondrial integrity and mitochondria-initiated cytochrome c release and caspase activation (Youle and Strasser 2008; Vogler 2012). Similarly, BIRC2 is described to be highly expressed following peripheral nerve injury (Wang et al. 2012). Our results showed that the expression of BCL2, BCL2L1 and BIRC2 anti-apoptotic genes was up-regulated by α-CYPER (3.62-, 2.85- and 3.17-fold, respectively), leading to incapacity to prevent caspase activation (Earnshaw et al. 1999). Moreover, exposure to α-CYPER

induced apoptotic cell death in SH-SY5Y cells by up-regulation of the representative pro-apoptotic genes including APAF1, CASP3, CASP7 and CASP9 (>twofold), which means that both intrinsic and extrinsic apoptosis pathways were activated by this pyrethroid (Li et al. 1997; Zimmermann et al. 2001; Yoshida 2003). Caspase-3 (CASP3) is a downstream effecter of caspase-9 (CASP9) and plays a critical role in the execution of apoptosis (Jänicke et al. 1998). Because a fragment of APAF1 can facilitate CASP9 activation (in this study 3.70-fold), the upregulation of APFA1 by α-CYPER might merit further study. Activated caspases cleave a variety of intracellular polypeptides, components of the DNA repair machinery and protein kinases and scissions that characterize the apoptotic cell death. Previously, it was observed that cypermethrin also induced apoptosis via caspase pathway (Jin et al. 2011a; Tiwari et al. 2012). On the other hand, the tumor suppressor TP53 which plays a vital role in safeguarding the integrity of the genome and regulates both apoptosis and autophagy was down-regulated by α-CYPER (−2.29-fold). In contrast, GADD45A, a stress sensor protein, exhibited the maximal overexpression (7.09-fold) after α-CYPER treatment. GADD45A plays a pivotal role as a stress sensor that modulates cellular response to a variety of stress conditions, including genotoxic and oncogenic stress (Cretu et al. 2009). Also, this study showed that α-CYPER induced FAS overexpression (7.65-fold) which might reflect alterations in the cytokine profile (Aschkenazi et al. 2002). Collectively, the changes of protein expressions before mentioned disrupt survival pathways and disassemble important architectural components of the cell, contributing to the morphological and biochemical changes that characterize apoptotic cell death.

Autophagy is an intracellular catabolic system that delivers cytoplasmic contents (e.g., proteins, lipids and organelles) to lysosomes for degradation. When cells encounter environmental stresses, such as nutrient starvation, hypoxia, oxidative stress and pathogen infection, the level of autophagy can be dramatically augmented as a cytoprotective response, resulting in adaptation and survival; however, deregulated or excessive autophagy may lead to cell death. In certain contexts, autophagy and apoptosis are in a fine balance. Thus, small perturbations in the signaling of one or other process can, under certain stress conditions, be enough to completely change the fate of the cell. Several families of proteins have been identified in mammalian autophagy regulation. Our results showed that α-CYPER overexpressed ULK1 (6.50-fold), a key complex required for autophagosome formation (Wirth et al. 2013). Also α-CYPER caused an upregulation of the autophagy marker proteins MAP1LC3A (3.24-fold), ATG5 (2.54-fold), ATG7 (3.87-fold) and ATG12 (2.12-fold) (Kim et al. 2013). Furthermore, there is an interrelationship between autophagy and apoptosis regulated by MAPK8 and BCL-2

phosphorylation (Yang and Klionsky 2010). In the present study, we observed that MAPK8 was up-regulated (>1.5-fold). Autophagy signaling process is also related to up-regulation of NFKB1, SNCA and SQSTM1 genes (Trocoli and Djavaheri-Mergny 2011; Dansithong et al. 2015; Jiang et al. 2015). In the present study, we observed over-expression of NFKB1 (4.41-fold), SNCA (4.68-fold) and SQSTM1 (3.04-fold). In conclusion, we demonstrated that mRNA levels of some key genes related to cell autophagy were significantly altered in α-CYPER-treated neuroblastoma SH-SY5Y cells.

While apoptosis is known as a regulated cellular mechanism, necrosis is known as passive cell death caused by overwhelming stress. Necrosis is characterized by rapid loss of plasma membrane integrity, organelle swelling and mitochondrial dysfunction, and the lack of typical apoptotic features such as internucleosomal DNA cleavage and nuclear condensation (Hitomi et al. 2008). Interestingly, it was discovered that in certain cell types, the activation of death receptors may lead to cell death with features of either apoptosis or necrosis argued for the existence of a regulated cellular necrosis mechanism termed necroptosis (Degterev et al. 2005). Our study showed that α-CYPER differentially altered expressions (fold changes, see Table 1) of BMF, COMMD4, HSPBAP1, JPH3, PARP1, PARP2, TXNLA4B genes related to TNFα-induced necroptosis (Hitomi et al. 2008). For this group of genes, the major overexpression (5.15-fold) was observed for JPH3 protein. Studies have demonstrated that the family of these junctophilins proteins (JP) takes part in the formation of the junctional membrane structure in excitable cells (Nishi et al. 2003) and JPH3 could contribute to α-CYPER neurotoxicity. On the other hand, it has been widely accepted that GABAergic mechanism is involved in the occurrence of seizure, and the inhibitory function of GABAergic is associated with the activity pattern of generalized seizures (Amabeoku and Farmer 2005; Su et al. 2008). Exposure to Type II pyrethroids, such as α-CYPER, is known to interact with the GABA receptor–ionophore complex and to induce neurological symptoms (Lawrence and Casida 1983; Lawrence et al. 1985). In this study, among α-CYPER-altered genes related to necrotic cell death, HSPABP1 is considered as potential modulator to GABAergic system (Xi et al. 2007; Xiong et al. 2009). HSPABP1 was found extensively in the cytoplasm of neurons and glial cells in patients with epilepsy (Xi et al. 2007). Our results showed that expression levels of HSPABP1 gene were significantly up-regulated in the cells exposed to α-CYPER to levels of 3.42 times greater than those in control cultures. Our HSP-ABP1 gene expression data suggest that this family may play a role in the development of seizures presented after α-CYPER exposure in mammals. Nevertheless, future studies are needed to confirm this hypothesis and to determine

whether α-CYPER acts directly or indirectly on this gene expression.

Taken together, the results of the present study in neuroblastoma SH-SY5Y cells provide insights concerning molecular mechanisms involved in the toxicity of α-CYPER. The findings indicate that α-CYPER induces cytotoxicity in SH-SY5Y cells via oxidative stress and apoptotic, autophagy and necrotic pathways.

Compliance with ethical standards

Conflict of interest The authors declare that there are no conflicts of interest

References

Aldridge WN (1990) An assessment of the toxicological properties of pyrethroids and their neurotoxicity. Crit Rev Toxicol 21:89–104

Amabeoku GJ, Farmer CC (2005) Gamma-aminobutyric acid and mefloquine-induced seizures in mice. Prog Neuropsychopharmacol Biol Psychiatry 29:917–921

Amer SM, Ibrahim AAES, El-Sherbeny KM (1993) Induction of chromosomal aberrations and sister chromatid exchange in vivo and in vitro by the insecticide cypermethrin. J Appl Toxicol 13:341–345

Anadón A, Martínez-Larrañaga MR, Martínez MA (2009) Use and abuse of pyrethrins and synthetic pyrethroids in veterinary medicine. Vet J 182:7–20

Anadón A, Ares I, Martínez MA, Martínez-Larrañaga MR (2013a) Pyrethrins and synthetic pyrethroids: use in veterinary medicine. In: Ramawat KG, Merillon JM (eds) Handbook of natural products. Springer, Berlin, pp 1–25. doi:10.10007/978-3-642-22144-6_131

Anadón A, Martínez M, Martínez M, Castellano V, Ares I, Romero A, Fernández R, Martínez-Larrañaga MR (2013b) Differential induction of cytochrome P450 isoforms and peroxisomal proliferation by cyfluthrin in male Wistar rats. Toxicol Lett 220:135–142

Aschkenazi S, Straszewski S, Verwer KMA, Foellmer H, Rutherford T, Mor G (2002) Differential regulation and function of the Fas/Fas ligand system in human trophoblast cells. Biol Reprod 66:1853–1861

Bauche F, Stephan JP, Touzalin AM, Jegou B (1998) In vitro regulation an inducible-type NO synthase in the rat seminiferous tubule cells. Biol Reprod 58:431–438

Casco VH, Izaguirre MF, Marin L, Vergara MN, Lajmanovich RC, Peltzer P, Soler AP (2006) Apoptotic cell death in the central nervous system of *Bufo arenarum* tadpoles induced by cypermethrin. Cell Biol Toxicol 22:199–211

Cort W, Scott J, Araujo M, Mergens W, Cannalonga M, Osadca M, Harley H, Parrish D, Pool W (1975) Antioxidant activity and stability of 6-hydroxy-2, 5, 7, 8-tetramethylchroman-2-carboxylic acid. J Am Oil Chem Soc 52:174–178

Cretu A, Sha X, Tront J, Hoffman B, Liebermann D (2009) Stress sensor Gadd45 genes as therapeutic targets in cancer. Can Ther 7:268–276

Dansithong W, Paul S, Scoles DR, Pulst SM, Duong P, Huynh DP (2015) Generation of SNCA cell models using zinc finger nuclease (ZFN) technology for efficient high-throughput drug screening. PLoS ONE 10(8):e0136930

Degterev A, Huang Z, Boyce M, Li Y, Jagtap P, Mizushima N, Cuny GD, Mitchison TJ, Moskowitz MA, Yuan J (2005) Chemical inhibitor of nonapoptotic cell death with therapeutic potential for ischemic brain injury. Nat Chem Biol 1:112–119

Denizot F, Lang R (1986) Rapid colorimetric assay for cell growth and survival: modifications to the tetrazolium dye procedure giving improved sensitivity and reliability. J Immunol Methods 89:271–277

Earnshaw WC, Martins LM, Kaufmann SH (1999) Mammalian caspases: structure, activation, substrates and functions during apoptosis. Annu Rev Biochem 68:383–424

Elwan MA, Richardson JR, Guillot TS, Caudle WM, Miller GW (2006) Pyrethroid pesticide-induced alterations in dopamine transporter function. Toxicol Appl Pharmacol 211:188–197

Giray B, Gürbay A, Hincal F (2001) Cypermethrin-induced oxidative stress in rat brain and liver is prevented by vitamin E or allopurinol. Toxicol Lett 118:139–146

Giri S, Giri A, Sharma GD, Prasad SB (2003) Induction of sister chromatid exchanges by cypermethrin and carbosulfan in bone marrow cells of mice in vivo. Mutagenesis 18:53–58

Hitomi J, Christofferson DE, Ng A, Yao J, Degterev A, Xavier RJ, Yuan J (2008) Identification of a molecular signaling network that regulates a cellular necrotic cell death pathway. Cell 135:1311–1323

Jänicke RU, Sprengart ML, Wati MR, Porter AG (1998) Caspase-3 is required for DNA fragmentation and morphological changes associated with apoptosis. J Boil Chem 17:9357–9360

Jiang T, Harder B, Rojo de la Vega M, Wong PK, Chapman E, Zhang DD (2015) p62 links autophagy and Nrf2 signaling. Free Radic Biol Med 88:199–204

Jin Y, Zheng S, Fu Z (2011a) Embryonic exposure to cypermethrin induces apoptosis and immunotoxicity in zebrafish (*Danio rerio*). Fish Shellfish Immun 30:1049–1054

Jin Y, Zheng S, Pu Y, Shu L, Sun L, Liu W, Fu Z (2011b) Cypermethrin has the potential to induce hepatic oxidative stress, DNA damage and apoptosis in adult zebrafish (*Danio rerio*). Chemosphere 82:398–404

Jin Y, Wang L, Ruan M, Liu J, Yang Y, Zhou C, Xu B, Fu Z (2011c) Cypermethrin exposure during puberty induces oxidative stress and endocrine disruption in male mice. Chemosphere 84:124–130

Kale M, Rathore N, John S, Bhatnagar D (1999) Lipid peroxidative damage on pyrethroid exposure and alterations in antioxidant status in rat erythrocytes: a possible involvement of reactive oxygen species. Toxicol Lett 105:197–205

Kim SH, Hwang SY, Min KS, Yoon JT (2013) Molecular cloning and expression analyses of porcine MAP1LC3A in the granulosa cells of normal and miniature pig. Reprod Biol Endocrinol 11:2–8

Kovalevich J, Langford D (2013) Considerations for the use of SH-SY5Y neuroblastoma cells in neurobiology. Chapter 2. In: Amini S, White MK (eds) Neuronal cell culture: methods and protocols, methods in molecular biology, vol 1078. Springer Science, New York, pp 9–20. doi:10.1007/978-1-62703-640-5_2

Lawrence LJ, Casida JE (1983) Stereospecific action of pyrethroids insecticides on the gamma-aminobutyric acid receptor-ionophore complex. Science 221:1399–1401

Lawrence LJ, Gee KW, Yamamura HI (1985) Interactions of pyrethroid insecticides with chloride ionophore associated binding sites. Neurotoxicology 6:87–98

Li P, Nijhawan D, Budihardjo I, Srinivasula SM, Ahmad M, Alnemri ES, Wang X (1997) Cytochrome c and dATP-dependent formation of Apaf-1/caspase-9 complex initiates an apoptotic protease cascade. Cell 91:479–489

Li H-Y, Wu S-Y, Shi N (2007) Transcription factor Nrf2 activation by deltamethrin in PC12 cells: involvement of ROS. Toxicol Lett 171:87–98

Malkiewicz K, Koteras M, Folkesson R, Brzezinski J, Winblad B, Szutowski M, Benedikz E (2006) Cypermethrin alters glial fibrillary acidic protein levels in the rat brain. Environ Toxicol Pharmacol 21:51–55

Mansour SA, Mossa ATH (2010) Oxidative damage, biochemical and histopathological alterations in rats exposed to chlorpyrifos and the antioxidant role of zinc. Pestic Biochem Physiol 96:14–23

Maurya SK, Rai A, Rai NK, Deshpande S, Jain R, Mudiam MKR, Prabhakar YS, Bandyopadhyay S (2012) Cypermethrin induces astrocyte apoptosis by the disruption of the autocrine/paracrine mode of epidermal grow factor receptor signaling. Toxicol Sci 125:473–487

Moncada S, Palmer RMJ, Higgs EA (1991) Nitric oxide: physiology, pathophysiology and pharmacology. Pharmacol Rev 43:109–142

Mun JY, Lee WY, Han SS (2005) Effects of cypermethrin on the dopaminergic neurons in the progressive hemiparkinsinian rats. Toxicol Mech Methods 15:399–404

Narahashi T (1996) Neuronal ion channels as the target sites of insecticides. Pharmacol Toxicol 79:1–14

Nasuti C, Gabbianelli R, Falcioni ML, Di Stefano A, Sozio P, Cantalamessa F (2007) Dopaminergic system modulation, behavioral changes, and oxidative stress after neonatal administration of pyrethroids. Toxicology 229:194–205

Nishi M, Sakagamib H, Komazakic S, Kondob H, Takeshimaa H (2003) Coexpression of junctophilin type 3 and type 4 in brain. Mol Brain Res 118:102–110

Pahlman S (1990) Human neuroblastoma cells in culture: a model for neuronal cell differentiation and function. Acta Physiol Scand 592:25–37

Pandi-Perumal SR, Srinivasan V, Maestroni GJM, Cardinali DP, Poeggeler B, Hardeland R (2006) Melatonin. Nature's most versatile biological signal? FEBS J 273:2813–2832

Patel S, Pandey A, Bajpayee M, Parmar D, Dhawan A (2006) Cypermethrin-induced DNA damage in organs and tissues of the mouse: evidence from the comet assay. Mutat Res 607:176–183

Power LE, Sudakin DL (2007) Pyrethrin and pyrethroid exposures in the United States: a longitudinal analysis of incidents reported to poison centers. J Med Toxicol 3:94–99

Raszewski G, Lemieszek MK, Lukawski K, Juszczak M, Rzeski W (2015) Chlorpyrifos and cypermethrin induce apoptosis in human neuroblastoma cell line SH-SY5Y. Basic Clin Pharmacol Toxicol 116:158–167

Rodríguez C, Mayo JC, Sainz RM, Antolin I, Herrera F, Martín V, Reiter RJ (2004) Regulation of antioxidant enzymes: a significant role for melatonin. J Pineal Res 36:1–9

Romero A, Egea J, García AG, López MG (2010) Synergistic neuroprotective effect of combined low concentrations of galantamine and melatonin against oxidative stress in SH-SY5Y neuroblastoma cells. J Pineal Res 49:141–148

Romero A, Ramos E, Ares I, Castellano V, Martínez M, Martínez-Larrañaga MR, Anadón A, Martínez MA (2016) Fipronil sulfone induced higher cytotoxicity than fipronil in SH-SY5Y cells: protection by antioxidants. Toxicol Lett 252:42–49

Singh AK, Tiwari MN, Dixit A, Upadhyay G, Patel DK, Singh D, Prakash O, Singh MP (2011a) Nigrostriatal proteomics of cypermethrin-induced dopaminergic neurodegeneration: microglial activation-dependent and -independent regulations. Toxicol Sci 122:526–538

Singh P, Lata P, Patel S, Pandey AK, Jain SK, Shanker R, Dhawan A (2011b) Expression profiling of toxicity pathway genes by real-time PCR array in cypermethrin-exposed mouse brain. Toxicol Mech Method 21:193–199

Singh AK, Tiwari MN, Prakash O, Singh MP (2012a) A current review of cypermethrin-induced neurotoxicity and nigrostriatal dopaminergic neurodegeneration. Curr Neuropharmacol 10:64–71

Singh AK, Tiwari MN, Upadhyay G, Patel DK, Singh D, Prakash O, Singh MP (2012b) Long term exposure to cypermethrin induces nigrostriatal dopaminergic neurodegeneration in adult rats: postnatal exposure enhances the susceptibility during adulthood. Neurobiol Aging 33:404–415

Soderlund DM, Bloomquist JR (1989) Neurotoxic actions of pyrethroid insecticides. Annu Rev Entomol 34:77–96

Su T, Cong WD, Long YS, Luo AH, Sun WW, Deng WY, Liao WP (2008) Altered expression of voltage-gated potassium channel 4.2 and voltage-gated potassium channel 4-interacting protein, and changes in intracellular calcium levels following lithium-pilocarpine-induced status epilepticus. Neuroscience 157:566–576

Tiwari MN, Singh AK, Ahmad I, Upadhyay G, Singh D, Patel DK, Singh C, Prakash O, Singh MP (2010) Effects of cypermethrin on monoamine transporters, xenobiotic metabolizing enzymes and lipid peroxidation in the rat nigrostriatal system. Free Radical Res 44:1416–1424

Tiwari MN, Singh AK, Agrawal S, Gupta SP, Jyoti A, Shanker R, Prakash O, Singh MP (2012) Cypermethrin alters the expression profile of mRNAs in the adult rat striatum: a putative mechanism of postnatal pre-exposure followed by adulthood re-exposure-enhanced neurodegeneration. Neurotox Res 22:321–334

Trocoli A, Djavaheri-Mergny M (2011) The complex interplay between autophagy and NF-κB signaling pathways in cancer cells. Am J Cancer Res 1:629–649

USEPA (2013) Pyrethroids and Pyrethrins. http://www.epa.gov/oppsrrd1/reevaluation/pyrethroids–pyrethrins.html

Verschoyle R, Aldridge W (1980) Structure-activity relationships of some pyrethroids in rats. Arch Toxicol 45:325–329

Vijverberg HP, vanden Bercken J (1990) Neurotoxicological effects and the mode of action of pyrethroid insecticides. Crit Rev Toxicol 21:105–126

Vogler M (2012) BCL2A1: the underdog in the BCL2 family. Cell Death Differ 19:67–74

Wang Y, Tang X, Yu B, Gu Y, Yuan Y, Yao D, Ding F, Gu X (2012) Gene network revealed involvements of Birc2, Birc3 and Tnfrsf1a in anti-apoptosis of injured peripheral nerves. PLoS ONE 7(9):e43436. doi:10.1371/journal.pone.0043436

Wirth M, Joachim J, Tooze SA (2013) Autophagosome formation—the role of ULK1 and Beclin1–PI3KC3 complexes in setting the stage. Semin Cancer Biol 23:301–309

Xi ZQ, Sun JJ, Wang XF, Li MW, Liu XZ, Wang LY, Zhu X, Xiao F, Li JM, Gong Y, Guan LF (2007) HSPBAP1 is found extensively in the anterior temporal neocortex of patients with intractable epilepsy. Synapse 61:741–747

Xiong H, Xia K, Li B, Zhao G, Zhang Z (2009) KChIP1: a potential modulator to GABAergic system. Acta Biochim Biophys Sin (Shanghai) 41:295–300

Xu C, Wu A, Zhu H, Fang H, Xu L, Jianxin Y, Shan J (2013) Melatonin is involved in the apoptosis and necrosis of pancreatic cancer cell line SW-1990 via modulating of BCL-2/BAX balance. Biomed Pharmacother 67:133–139

Yang Z, Klionsky DJ (2010) Mammalian autophagy: core molecular machinery and signaling regulation. Curr Opin Cell Biol 22:124–131

Yoshida H (2003) The role of apaf-1 in programmed cell death: from worm to tumor. Cell Struct Funct 28:3–9

Youle RJ, Strasser A (2008) The BCL-2 protein family: opposing activities that mediate cell death. Nat Rev Mol Cell Biol 9:47–59

Zhao M, Zhang Y, Wang C, Fu Z, Liu W, Gan J (2009) Induction of macrophage apoptosis by an organochlorine insecticide acetofenate. Chem Res Toxicol 22:504–510

Zimmermann KC, Bonzon C, Green DF (2001) The machinery of programmed cell death. Pharmacol Ther 92:57–70